Earthline Journal of Chemical Sciences
E-ISSN: 2581-9003; CODEN: EJCSB4
Volume 12, Number 1, 2025, Pages 47-64
https://doi.org/10.34198/ejcs.12125.047064

Some isomers of boron-nitrogen doped phenanthrene – DFT treatment

Lemi Türker

Department of Chemistry, Middle East Technical University, Üniversiteler, Eskişehir Yolu No: 1, 06800 Çankaya/Ankara, Turkey
e-mail: lturker@gmail.com; lturker@metu.edu.tr

Abstract

Phenanthrene is an even alternant aromatic hydrocarbon. In adjacent positions simultaneously boron and nitrogen doped phenanthrene and some of their derivatives have found some technological applications. In the present study, isomers of phenanthrene perturbed as mentioned above have been considered within the restrictions of density functional theory at the level of B3LYP/6-311++G(d,p) level. All the isomeric structures presently considered are thermally favored and electronically stable at the standard states. Various structural and quantum chemical data have been collected and discussed, including UV-VIS spectra. Also the NICS (0) data have been obtained for the isomers.

1. Introduction

Aromatic systems having cyclic conjugation of π-electrons provide ample possibilities in science and technology. In the classical theory, the presence of Clar's sextet(s) [1] in aromatic structures allows emergence of some localized double bonds. Phenanthrene is one of those structures having two Clar's sextets and one localized double bond [2]. Although, phenanthrene anthracene etc., are interesting structures from many points of views some centric perturbations [3-5] make them more interesting and in some cases very potential compounds to be used technologically. The boron and nitrogen replacement of carbon atoms (centric perturbation) in benzene π-system results in borazine. The Pauling electro negativities of carbon, boron and nitrogen atoms are 2.6, 2.0 and 3.0, respectively [6]. Borazine, (also known as borazole, $B_3H_6N_3$,) is an inorganic compound which possesses, the alternate three BH units and three NH units. The compound is isostructural and isoelectronic with benzene. The electron deficiency on the boron atom and the lone pair on nitrogen favor alternative mesomeric structures for borazine.

Polycyclic aromatic hydrocarbons (PAHs) with boron–nitrogen (BN) moieties have attracted tremendous interest due to their intriguing electronic and optoelectronic properties [7].

Due to its similarities to benzene, there have been a number of computational and experimental analyses of borazine's aromaticity. The number of pi-electrons in borazine obeys the 4n + 2 rule, and the B-N bond lengths are equal, which suggests the compound may be aromatic. The electronegativity difference between boron and nitrogen, however, creates an unequal sharing of charge which results in bonds with greater ionic character, and thus it is expected to have poorer delocalization of electrons than the all-carbon analog. Borazine, with a standard enthalpy change of formation $\Delta_f H$ of −531 kJ/mol, is thermally very stable [8].

As mentioned above, BN-embedded aromatic compounds have attracted great attention due to their fascinating properties resulted from the replacement of CC unit with isoelectronic BN unit in aromatics [9]. A

Received: October 21, 2024; Accepted: November 14, 2024; Published: November 16, 2024

Keywords and phrases: phenanthrene, boron and nitrogen substitution, DFT calculations, perturbations, NICS.

centric perturbation by an electronegative atom at suitable sites of a π-system which is isoconjugate with an alternant hydrocarbon lowers both the HOMO and LUMO energy levels of the isoelectronic system [3-5].

The stability and aromaticity of benzene, naphthalene, anthracene, tetracene, pentacene and their BN-analogs have been evaluated using density functional theory [10]. Enhanced stability has been found when B and N-atoms are adjacent to each other.

Boron-doped carbon materials have been experimentally and theoretically investigated from different perspectives, not only as anode materials for Li-ion batteries, but also towards other potential applications, such as high-temperature oxidation protectors for carbon/carbon (C/C) composites. Recently, heteroatom substitution into carbon materials has been addressed as a novel method for the enhancement of Li-ion capacities of carbon anodes. Many heteroatom-substituted carbon materials have been examined from experimental [11,12] and theoretical [13,14] viewpoints. BN- and B-doped systems attract most intense interest. The former are isoelectronic with the carbon precursors, while the latter are electron-deficient structures expected to be effective electron acceptors.

Tadjer et al., investigated boron–nitrogen- and boron-substituted anthracene and -phenanthrenes in order to developed models for doped carbon-based materials [15]. All-boron analogues of anthracene and phenanthrene was the interest of Sergeeva et al., [16]. Solid-state and solution phase reactivity of 10-hydroxy-10,9 boroxophenanthrene was studied by Philp et al., [17]. Lischka et al., investigated the biradicaloid nature of acenes by chemical doping with boron and nitrogen [18]. Wang et al., summarized the recent advances in boron - containing acenes [19].

Tunable properties and flexibility have made organic π-conjugated systems attractive targets for applications in organic light emitting diodes (OLEDs), [20,21] organic photovoltaics (OPVs), [22,23] and organic field-effect transistors (OFETs) [24,26].

Chen et al., reviewed the multiple-boron–nitrogen (multi-BN) doped π-conjugated systems for optoelectronics [27].

In the present study phenanthrene structure has been subjected to bicentric perturbations (BN unit), in such a way that at least one of the heteroatoms is at the fusion points of the rings with the exception of structure-1 (see Figure 1), and the perturbed structures have been treated in the realm of density functional theory to investigate the various quantum chemical properties.

2. Method of Calculations

In the present study, all the initial optimizations of the structures leading to energy minima have been achieved first by using MM2 method which is then followed by semi empirical PM3 self consistent fields molecular orbital method [28-30]. Afterwards, the structure optimizations have been achieved within the framework of Hartree-Fock and finally by using density functional theory (DFT) at the level of B3LYP/6-311++G(d,p) [31,32]. Note that the exchange term of B3LYP consists of hybrid Hartree-Fock and local spin density (LSD) exchange functions with Becke's gradient correlation to LSD exchange [33]. The correlation term of B3LYP consists of the Vosko, Wilk, Nusair (VWN3) local correlation functional [34] and Lee, Yang, Parr (LYP) correlation correction functional [35]. In the present study, the normal mode analysis for each structure yielded no imaginary frequencies for the $3N–6$ vibrational degrees of freedom, where N is the number of atoms in the system. This search has indicated that the structure of each molecule considered corresponds to at least a local minimum on the potential energy surface. Furthermore, all the bond lengths have been

thoroughly searched in order to find out whether any bond cleavage occurred or not during the geometry optimization process. All these computations were performed by using SPARTAN 06 [36]. Whereas the nucleus-independent chemical shift, NICS(0), calculations have been performed by using Gaussian 03 program [37].

3. Results and Discussion

Presently, boron and nitrogen bicentric perturbations carried out at the fusion points of rings-B and C of phenanthrene. Figure 1 shows labeling of the three rings in the isomers considered.

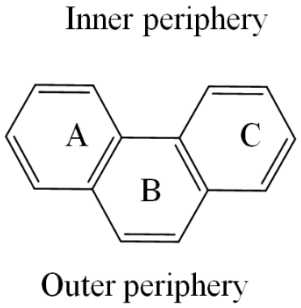

Figure 1. Labeling of the rings in the isomers considered.

Figure 2 shows the optimized structures and the direction of the dipole moment vectors of the isomers considered. As seen in the figure, in each structure either boron or nitrogen atom occupies the fusion points of

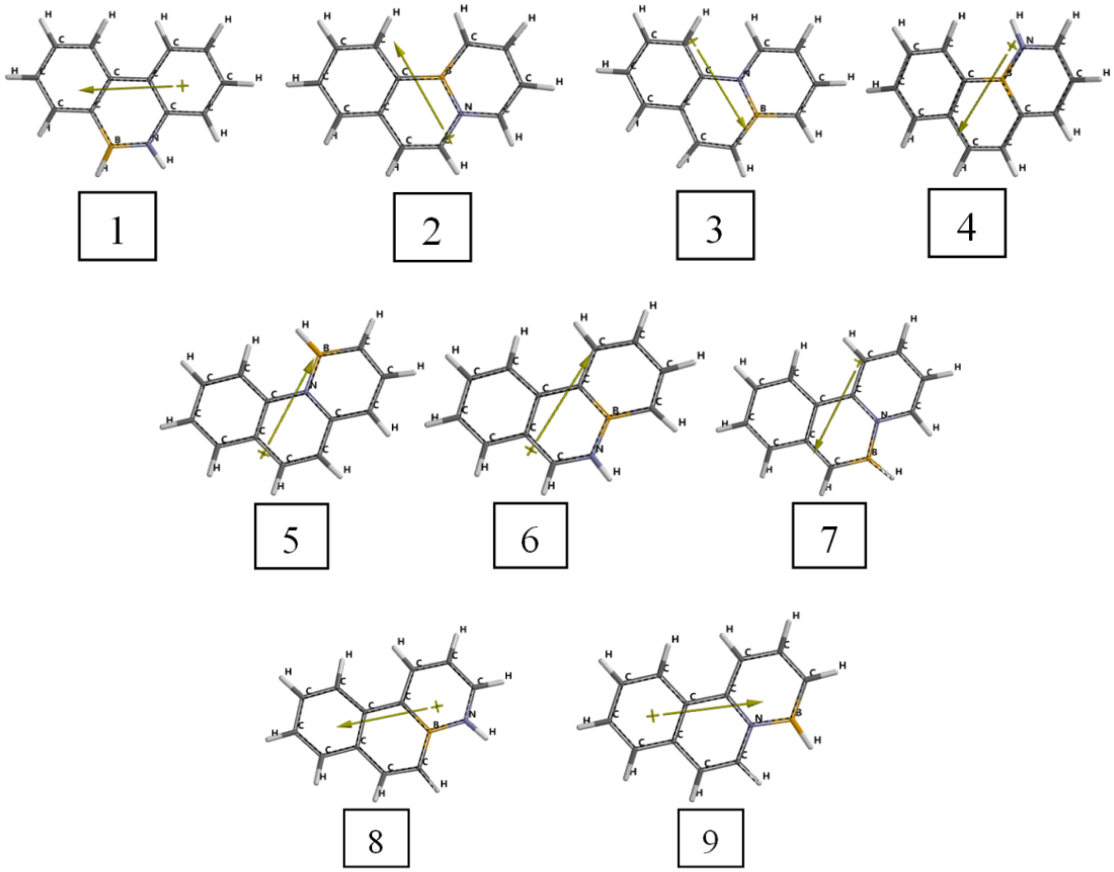

Figure 2. Optimized structures of the isomers considered.

the rings (B and C-rings). The other heteroatom of BN unit resides at the adjacent peripheral position. In structures-2 and 3 both of the heteroatoms occupy the fusion points whereas in the others only boron or nitrogen atom is at the fusion point. The direction of the dipole moment vector varies from structure to structure in the isomers. The dipole moment provides a measure of the extent to which charge distributed in a molecule. The magnitude of the dipole moment also depends on the extent to which charge is separated. All these factors dictate the magnitudes and the direction of the resultant dipole moments.

Table 1 displays some of the standard thermo chemical formation data of the isomers considered. The data reveal that the standard heat of formation (H^o) values of all the isomers are exothermic and they are favored according to their G^o values.

Table 1. Some thermo chemical properties of the isomers considered.

Isomer	Atom at the fusion point(s)	H^o	S^o (J/mol^o)	G^o
1	C	-1425435.295	390.50	-1425551.721
2	N, B	-1425387.920	391.86	-1425504.753
3	B,N	-1425372.266	391.53	-1425489.002
4	B	-1425410.769	392.56	-1425527.813
5	N	-1425349.952	390.18	-1425466.286
6	B	-1425370.097	392.29	-1425487.059
7	N	-1425324.508	390.39	-1425440.905
8	B	-1425403.541	392.42	-1425520.543
9	N	-1425357.135	390.19	-1425473.472

Energies in kJ/mol.

The algebraic order of H^o and G^o values is 1<4<8<2<3<6<9<5<7. Hence, simultaneous BN perturbation on adjacent sites decreases H^o and G^o depending on where the perturbation occurs. Comparing the values of structures-2 and 3 in which the same type of perturbation (BN) exists but topologically at different fusion sites (see Figure 1), one observes that boron in the inner periphery (structure-2) results more negative values. The data reveals that boron at the fusion point stabilizes (more exothermic and more favorable values) the structure better than nitrogen atom.

Table 2 shows some energies of the isomers considered where E, ZPE and E_C stand for the total electronic energy, zero point vibrational energy and the corrected total electronic energy, respectively. According to the data, they are all electronically stable structures. The stability order is 7<5<9<6<3<2<8<4<1. Hence, compared to phenanthrene molecule, BN perturbation destabilizes the structure at different extents depending on the fine topology of the perturbation site. Since octet hole of the boron atom is filled with the lone pair of the nitrogen atom, π-electron population of the ring should be less compared to the other ring which is unperturbed.

Table 2. Some energies of the isomers considered.

Isomer	Atom at the fusion point(s)	E	ZPE	E_C
1	C	-1425950.42	501.92	-1425448.50
2	BN	-1425904.14	503.06	-1425401.08
3	BN	-1425887.90	502.28	-1425385.62
4	B	-1425928.37	504.25	-1425424.12
5	N	-1425862.37	499.23	-1425363.14
6	B	-1425887.12	503.64	-1425383.48
7	N	-1425836.56	498.88	-1425337.68
8	B	-1425921.17	504.20	-1425416.97
9	N	-1425870.06	499.77	-1425370.29

Energies in kJ/mol.

Table 3 shows some calculated properties of the isomers presently considered. Note that a net dipole moment which is the vector sum of individual bond dipoles are a function of bond charges (charges on the atoms linked by the bond considered) and the bond distance. The order of dipole moments is 1<2<3<5<4<8<9<6<7.

The polarizability is defined according to a multivariable formula [36] which is the functions of van der Waals volume and hardness, respectively. The later one is dictated by energies of the highest occupied (HOMO) and the lowest unoccupied (LUMO) molecular orbitals [36]. Consequently, the polarizability order becomes 1<3<2=8<4<9<5<6<7.

Table 3. Some properties of the isomers presently considered.

Isomer	Area (Å²)	Volume (Å³)	PSA (Å²)	Ovality	Cv (J/molº)	Polarizability	Dipole (debye)
1	207.81	201.25	10.243	1.25	145.03	56.57	1.00
2	209.71	202.75	0.494	1.26	144.05	56.72	1.45
3	207.75	202.18	0.539	1.25	144.98	56.70	1.49
4	209.28	201.35	10.399	1.26	144.62	56.80	2.26
5	207.74	202.32	0.569	1.25	144.84	56.89	2.25
6	207.88	201.05	10.673	1.25	145.30	56.90	3.23
7	207.98	202.48	0.516	1.25	145.14	57.02	3.30
8	207.91	201.07	10.711	1.25	145.00	56.72	2.42
9	208.32	202.56	0.517	1.25	144.75	56.87	2.49

The calculated area and volume values of the isomers change from one isomer to the other but close to each other. Ovalities or Cv values are almost the same. Variations in the polarizabilities occur in a small range.

Figure 3 shows the exposed areas of the atoms in the isomers considered (Hydrogens omitted). They are sensitive to electronic and topological changes. When the boron atom is on the periphery of the system, its exposed area is about 18-21 $Å^2$ but at the fusion points is 10-12 $Å^2$.

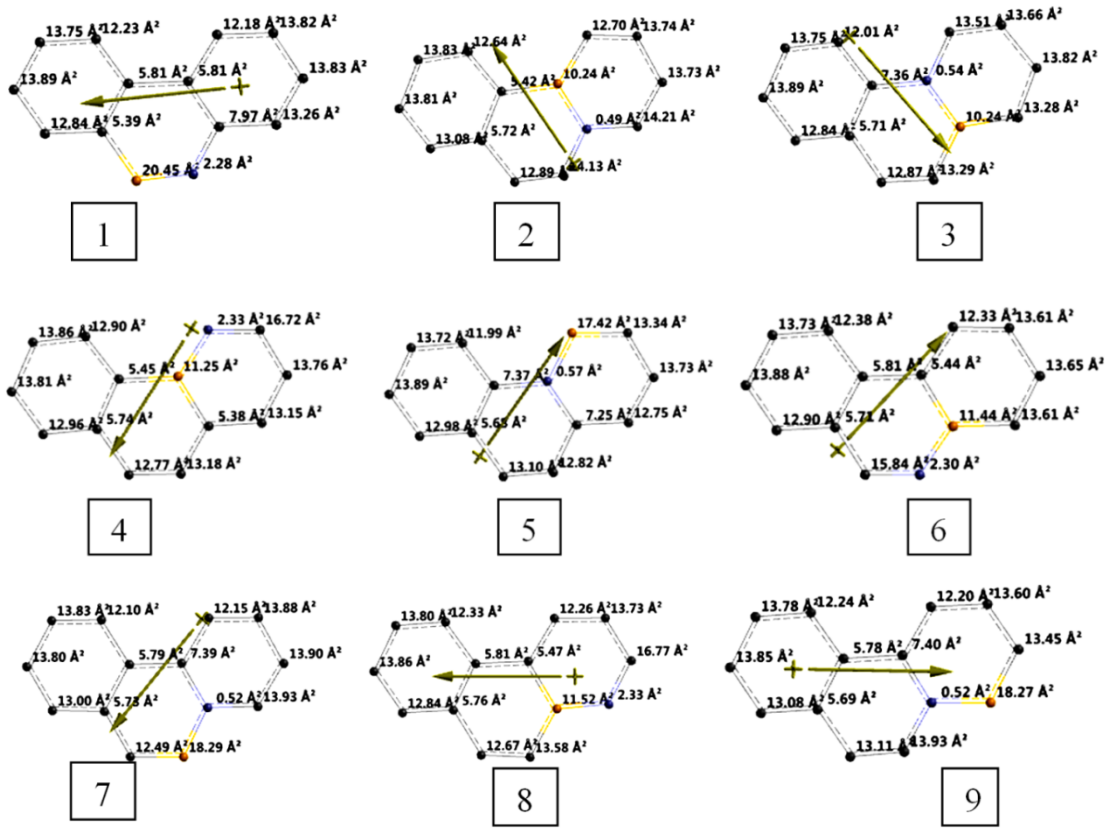

Figure 3. The exposed areas of the atoms in the isomers considered (Hydrogens omitted).

It is worth mentioning that the polar surface area (PSA) is defined as the amount of molecular surface area arising from polar atoms (N,O) together with their attached hydrogen atoms. Although these compounds are isomeric, their PSA values differ from each other meaning that the same kind of atoms might be influenced by electronic factors differently at different positions. Note that presently structures 2, 3, 5, 7 and 9 have comparatively much smaller PSA values than the others. All imply that fine (structural and electronic) topology of the isomers are implicitly but highly influential on magnitudes of the PSA values.

Figure 4 shows the ESP charges on atoms of the isomers considered. Note that the ESP charges are obtained by the program based on a numerical method that generates charges that reproduce the electrostatic potential field from the entire wavefunction [36]. The figure indicates that in all the cases, except isomers 7 and 9, the boron atom is positively charged. On the other hand, the nitrogen atom is positively charged in isomers 2,3,7 and 9 but negatively charged in the cases of isomers 1, 4, 5, 6 and 8. Of these negative charge acquired nitrogen atoms, only the one in isomer-5 resides on the fusion point. The direction of the dipole moment vector in this isomer is such that some electron population from ring-B and/or carbon atoms adjacent to the nitrogen is pulled towards the nitrogen atom because of its neighbor boron atom (see Figure 2).

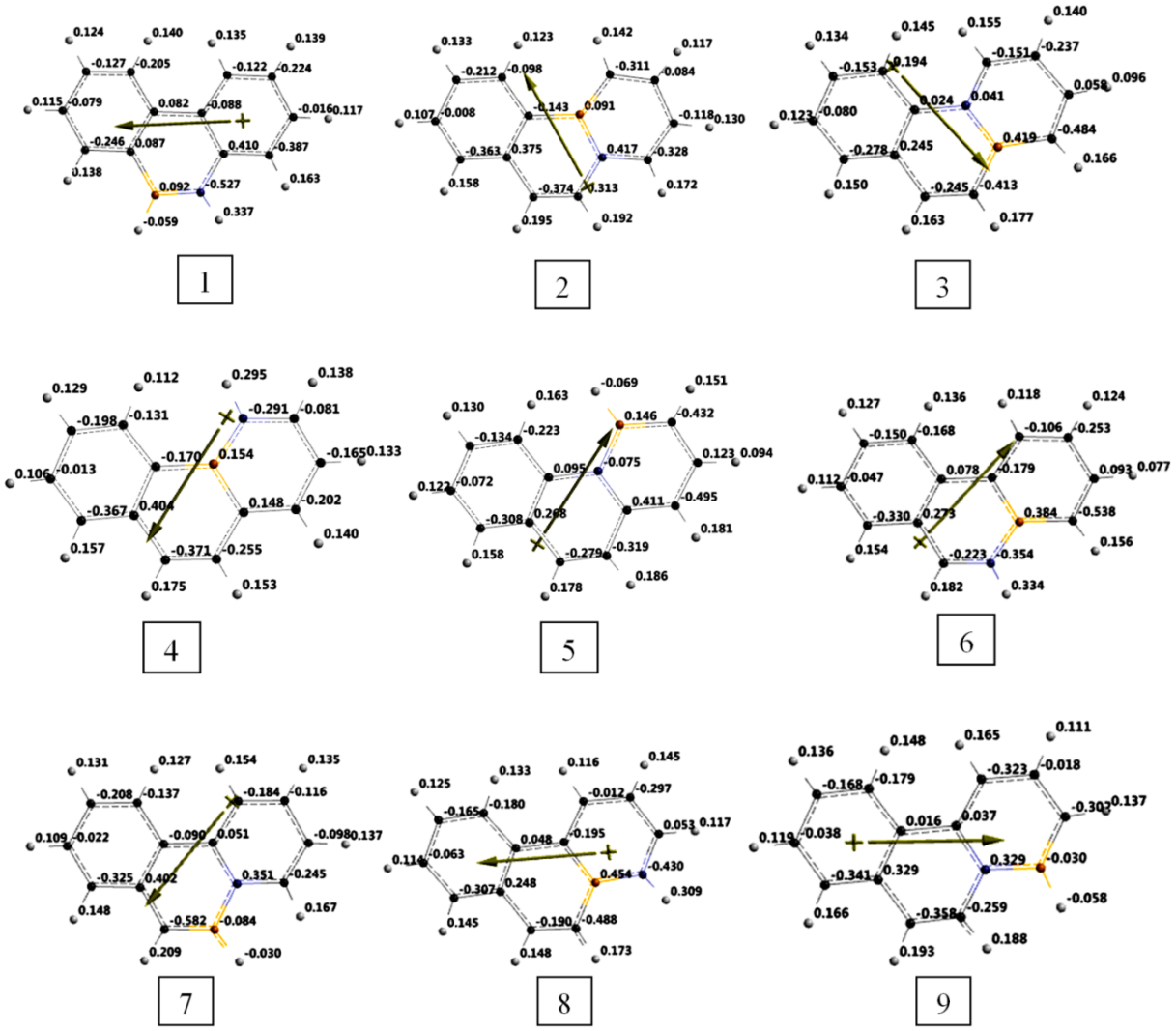

Figure 4. The ESP charges on atoms of the isomers considered.

Electrostatic potential is the energy of interaction of a positive charge with a molecule. It represents a balance between repulsive interactions involving the positively charged nuclei and attractive interactions involving the negatively charged electrons.

Figure 5 stands for the electrostatic potential maps of the isomers where negative potential regions reside on red/reddish and positive ones on blue/bluish parts of the maps. Electrostatic potential map paints the value of

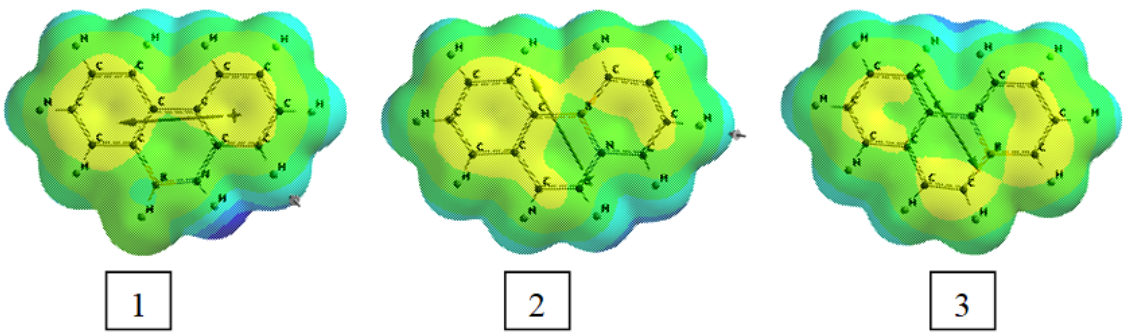

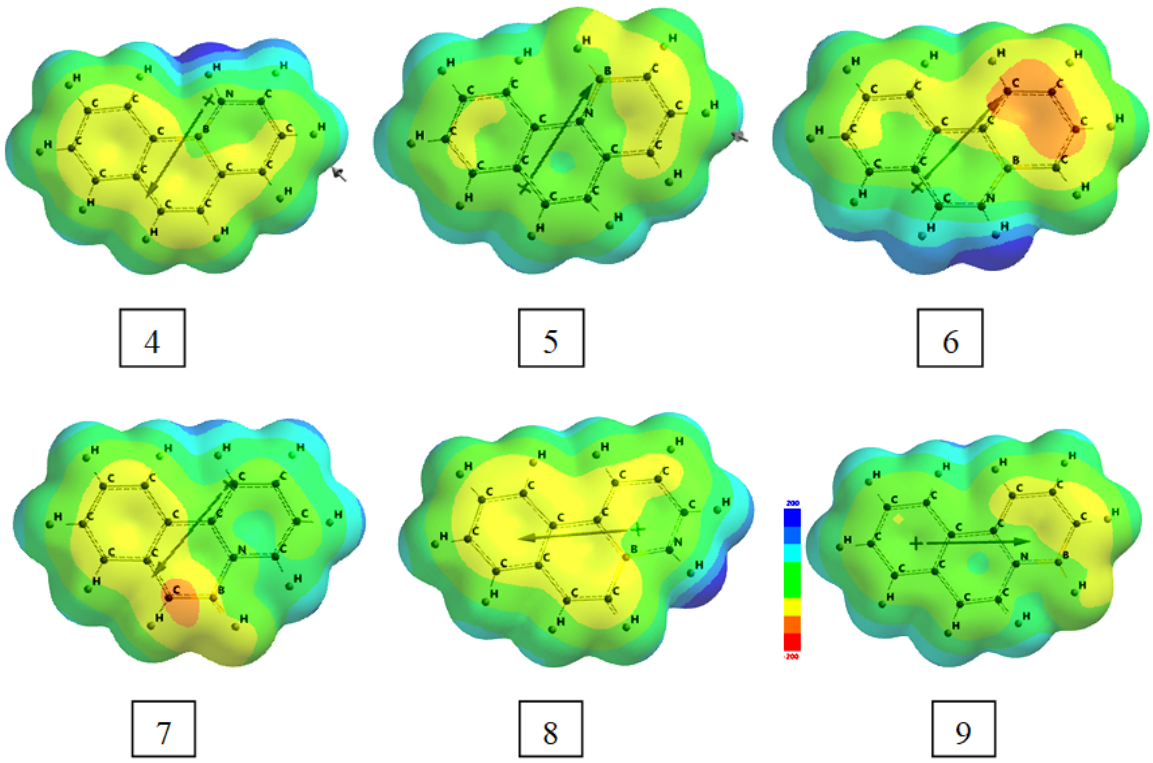

Figure 5. The electrostatic potential maps of the isomers.

electrostatic potential onto an electron density surface. Structure-6 possesses a highly intense negative potential region on the periphery of ring-C. Also structure-7 has a less intense small negative potential region in ring-A around carbon atom next to the boron atom. Probably some electron population accumulates there and thus the tip point of the dipole moment vector aims at there as in the case of structure-7 (see ring-C of it). Some positive potential exist, in varying strengths, around the peripheries of the isomers.

The local ionization potential maps of the isomers are shown in Figure 6, where conventionally red/reddish regions (if any exists) on the density surface indicate areas from which electron removal is relatively easy, meaning that they are subject to electrophilic attack. It is worth remembering that the local ionization potential map is a graph of the value of the local ionization potential on an isodensity surface corresponding to a van der Waals surface.

The LUMO maps of the isomers are shown in Figure 7. Note that a LUMO map displays the absolute value of the LUMO on the electron density surface. The blue color (if any exists) stands for the maximum value of the LUMO and the red colored region, associates with the minimum value. Note that the LUMO and NEXTLUMO are the major orbitals directing the molecule towards of the attack of nucleophiles [36]. Positions where the greatest LUMO coefficient exists is the most vulnerable site in nucleophilic reactions.

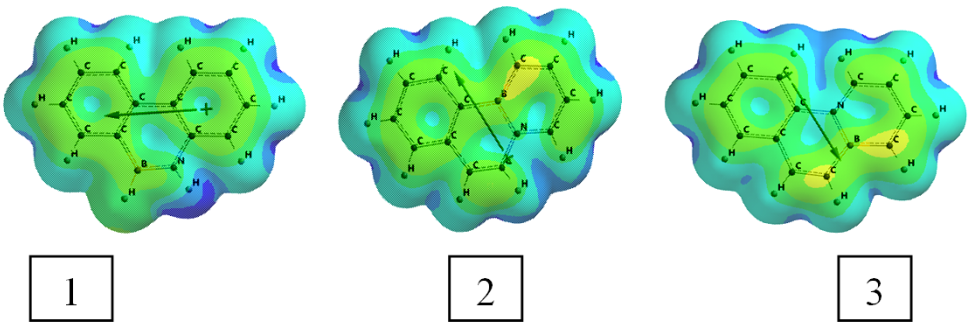

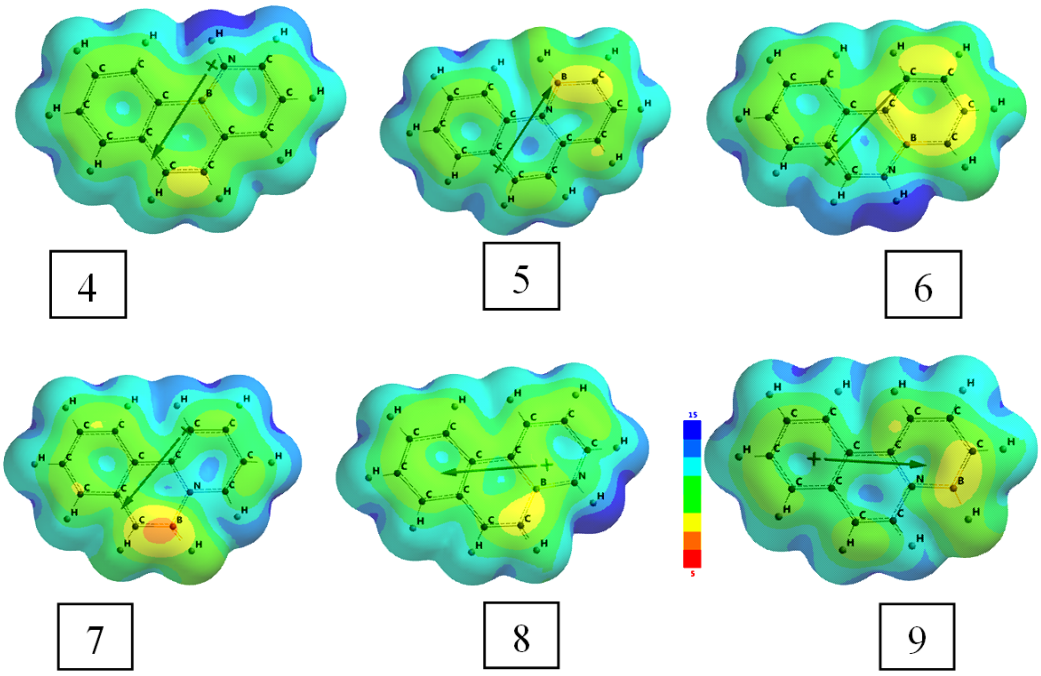

Figure 6. The local ionization potential maps of the isomers.

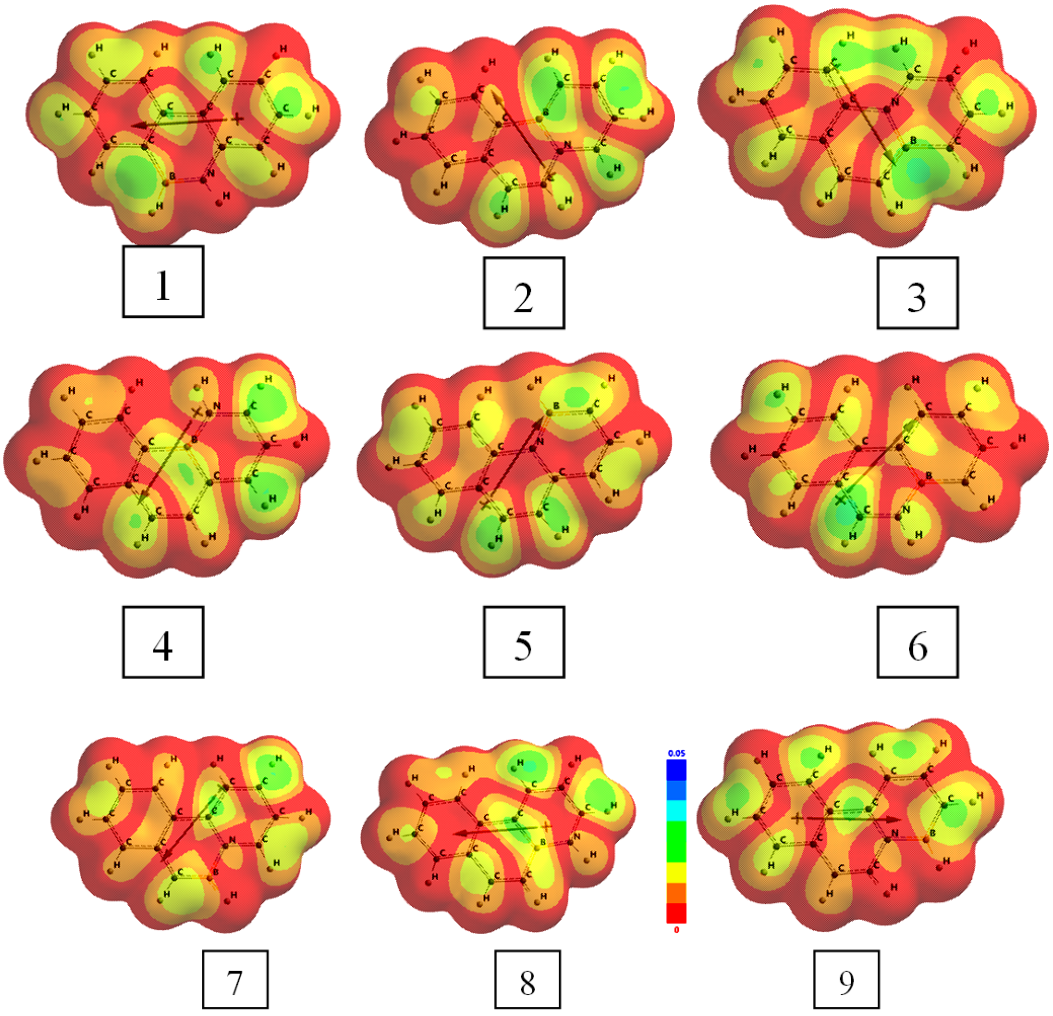

Figure 7. The LUMO maps of the isomers.

Figure 8 shows the bond densities of the isomers considered. The bond density contains fewer electrons in total and demarks atomic connectivity.

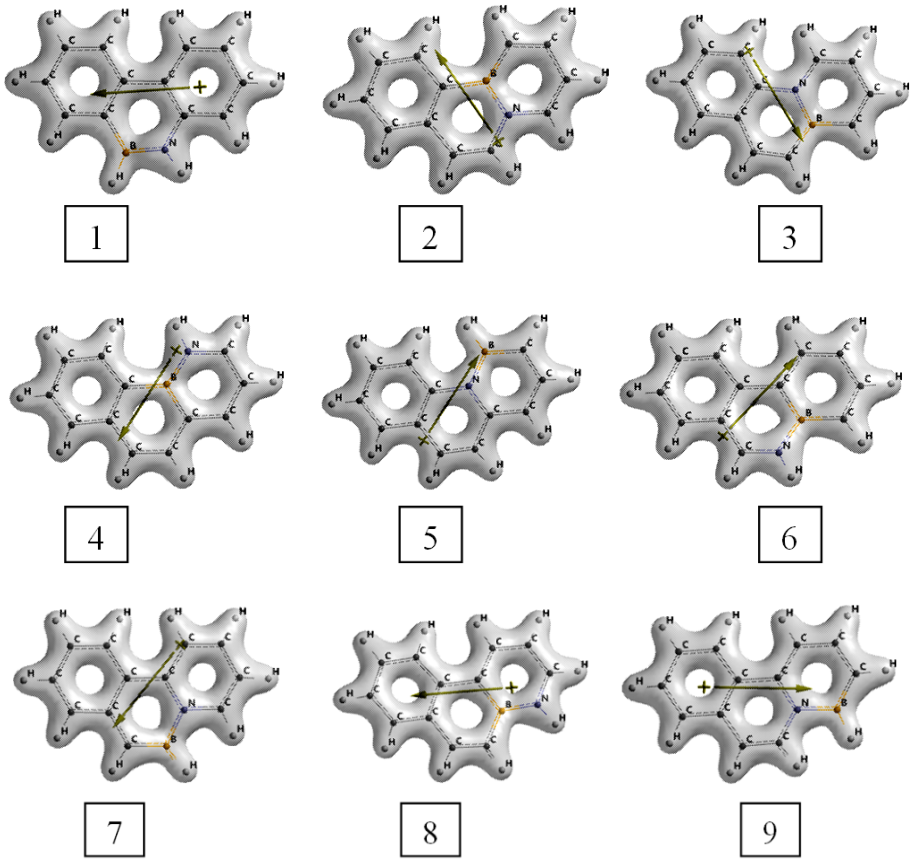

Figure 8. The bond densities of the isomers considered.

In the figure the perturbation effect of boron atom in every case is clearly discernable.

Table 4 lists the HOMO, LUMO energies and the interfrontier molecular orbital energy gap, Δε, values ($\Delta\varepsilon=\varepsilon_{LUMO}-\varepsilon_{HOMO}$) of the isomers considered.

Table 4. The HOMO, LUMO energies and Δε values of the isomers considered.

Isomer	Atom at the fusion point(s)	HOMO	LUMO	Δε
1	C	-592.91	-134.04	458.87
2	BN	-581.99	-133.85	448.14
3	BN	-591.77	-152.94	438.83
4	B	-543.00	-171.10	371.90
5	N	-543.81	-178.52	365.29
6	B	-527.92	-209.43	318.49
7	N	-503.97	-186.74	317.23
8	B	-562.69	-171.18	391.51
9	N	-547.56	-165.59	381.97

Energies in kJ/mol.

The order of the HOMO energies is 1<3<2<8<9<5<4<6<7 whereas the LUMO energies follow the order of 6<7<5<8<4<9<3<1<2. Consequently, the order of Δε values is 1>2>3>8>9>4>5>6>7. Note that phenanthrene is an even alternant hydrocarbon and nitrogen and boron at the starred positions should have opposite effects on the HOMO and LUMO energy levels [3,4]. The overall effect is dictated by intriguing topological and electronic factors.

Figure 9 displays the HOMO and LUMO patterns of the isomers considered. As it is evident from the figure all the HOMO and LUMO orbitals of the isomers possess π-symmetry and mostly are localized on two adjacent atoms only.

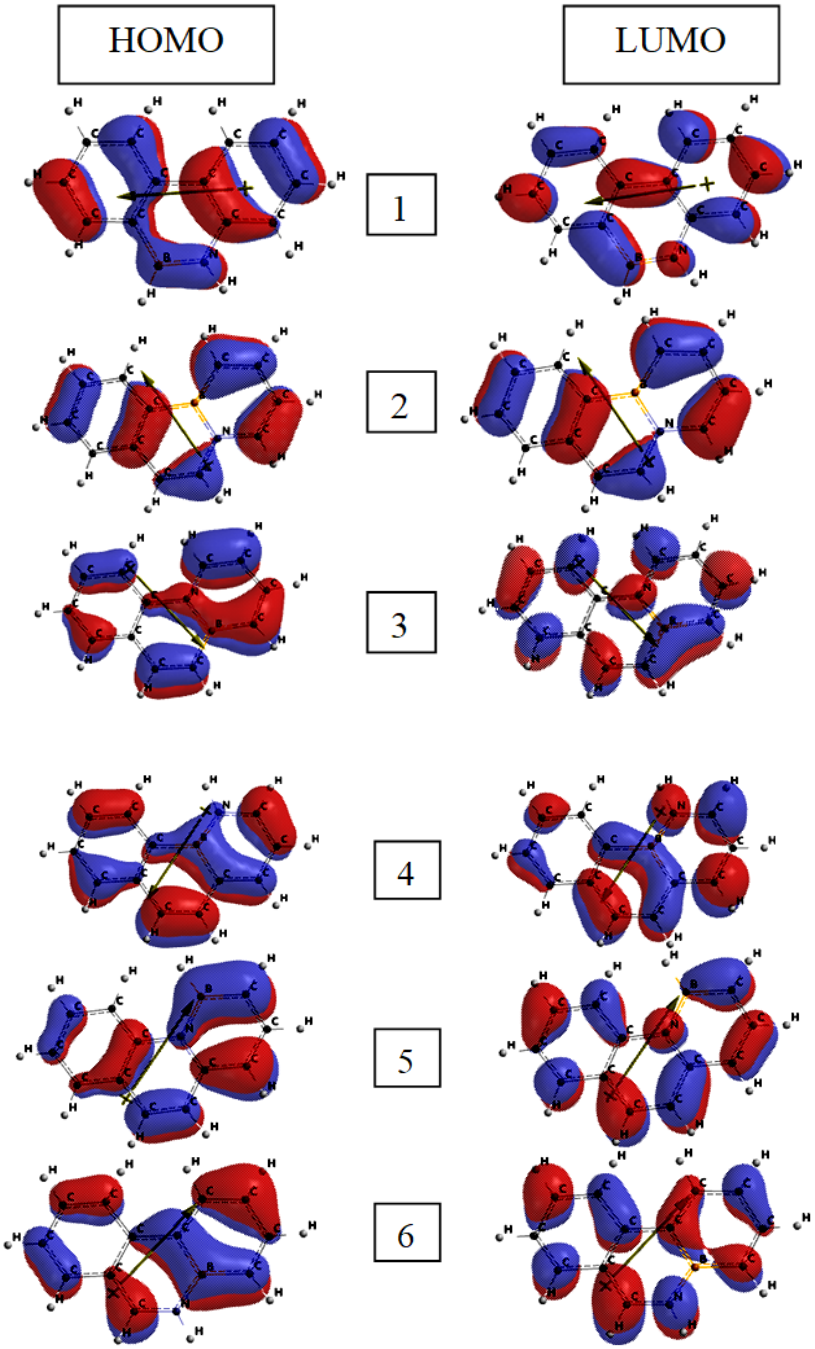

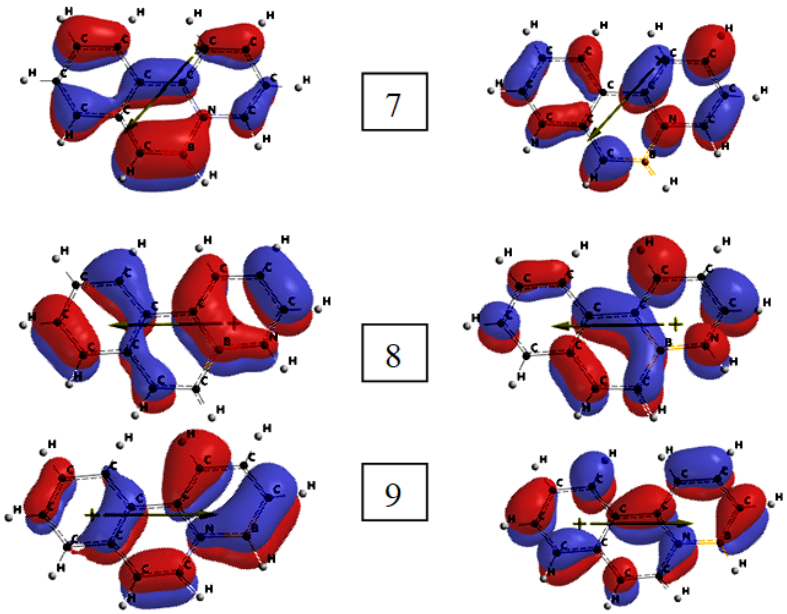

Figure 9. The HOMO and LUMO patterns of the isomers considered.

The calculated UV-VIS spectra (TDDFT) of the isomers are shown in Figure 10. As seen in the figure, going from isomer 1-3 the spectra are characterized with an emerging shoulder. In the cases of 4-7, the shoulder becomes a very discernable peak accompanied by a bathochromic effect [5,39]. Then, in isomers-8 and 9 the peaks are observable but a hypsochromic effect is observed [5,40].

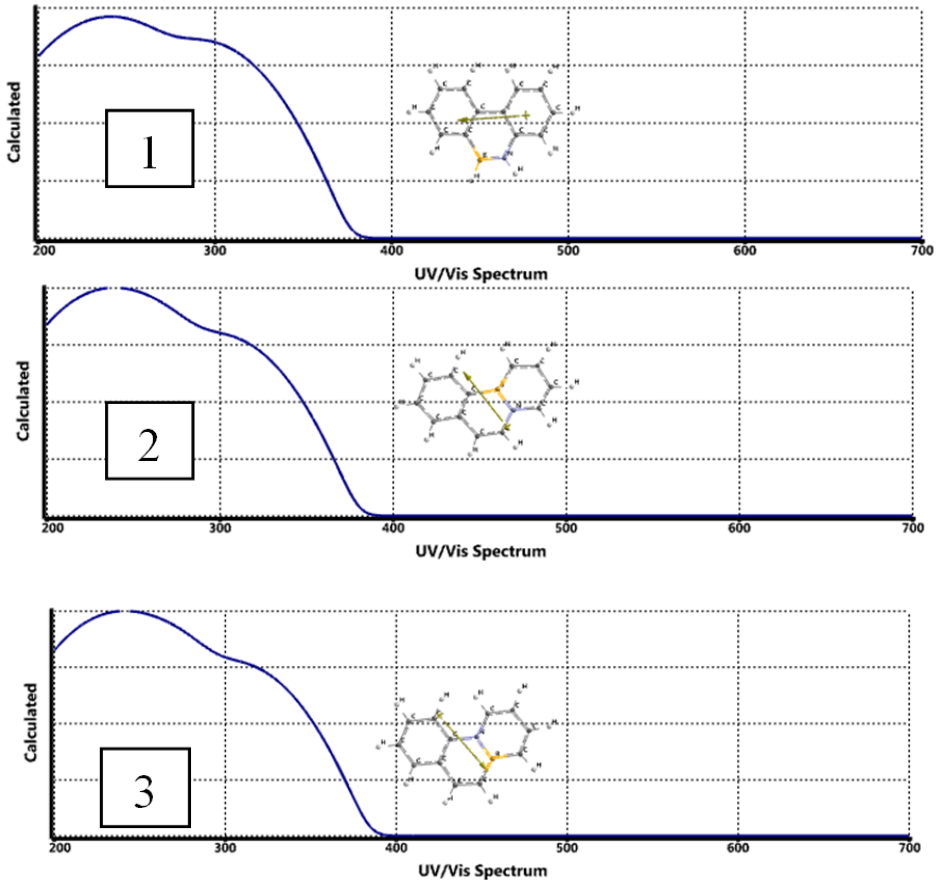

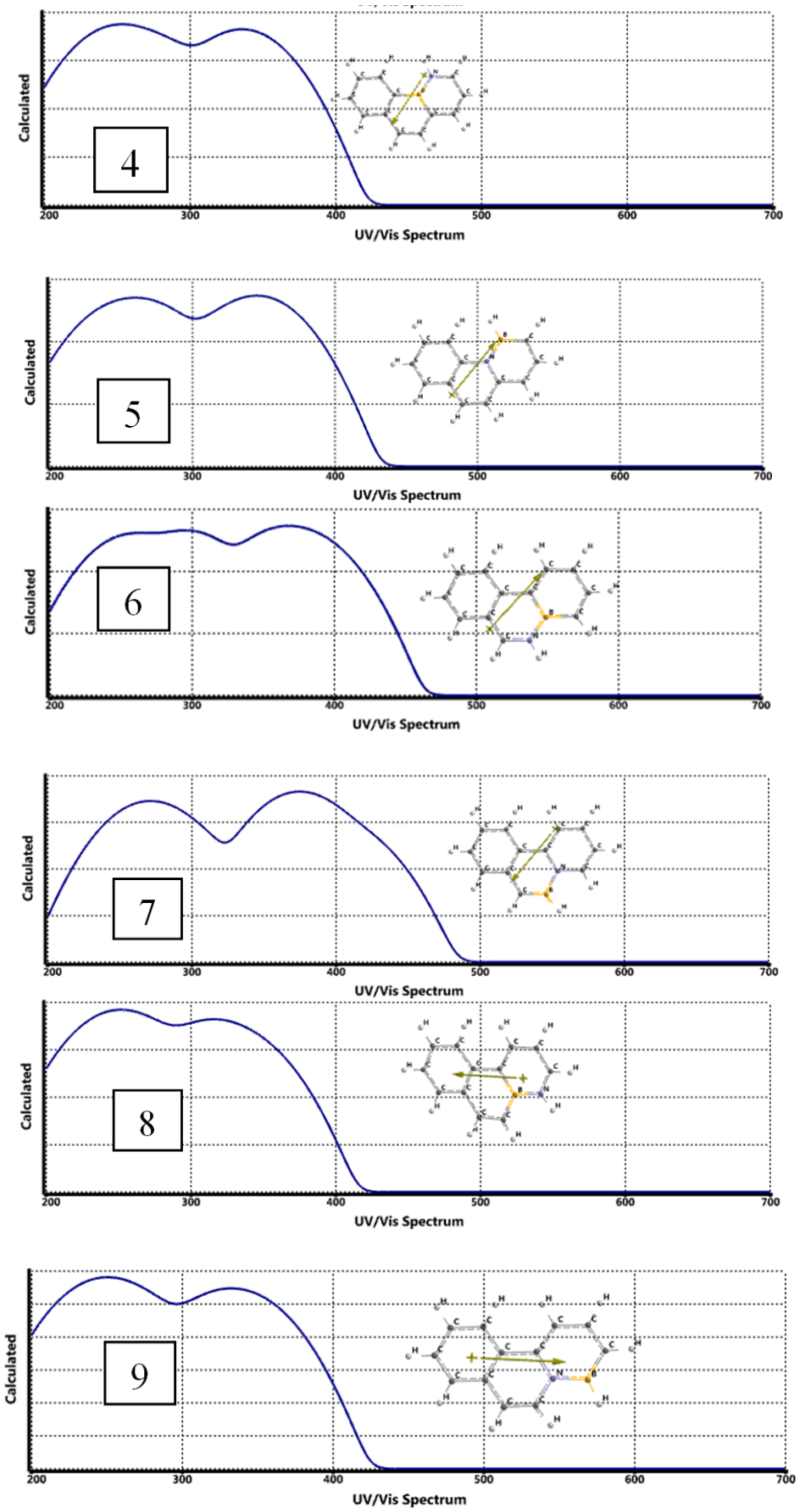

Figure 10. The calculated UV-VIS spectra (TDDFT) of the isomers considered.

Table 5 lists the calculated λ_{max} values (nm) of the isomers considered.

Table 5. The calculated λ_{max} values (nm) of the isomers considered.

1	2	3	4	5	6	7	8	9
231.62	233.76	234.68	250.17	249.14	257.13	270.37	248.02	247.13
245.70	252.29	243.11	277.07	269.05	297.99	374.59	254.77	262.84
293.96		259.05	335.80	346.18	361.16		313.18	323.25
					380.11			340.25

Table 6 displays "nucleus-independent chemical shift" NICS(0) values of the rings of the isomers considered. The calculated data so far have piled in the literature [41-52], have indicated that negative NICS values are associated with aromaticity. On the contrary, positive NICS values are associated with antiaromaticity while small NICS values are indicative of non-aromaticity. The data reveal that, with the exception of isomers-6 and 7, the NICS value of Ring-A is more negative than the respective value of either of the other rings. Also for those isomers, the NICS value of ring-C is more negative than the value of ring-B. Namely, in general (keeping the exceptional ones aside) the NICS values of the rings follow the algebraic order of A<C<B. Note that compared to carbocyclic analogs, any perturbation in the cyclic conjugation somewhat disturbs the homogeneity of the conjugation present (thus the Clar's sextet is affected).

Table 6. NICS(0) values of the rings of the isomers considered.

		Rings		
Isomer	Atom at the fusion point(s)	A	B	C
1	C	*	-1.6540	-6.3295
2	BN	-8.0112	-3.3258	-5.3131
3	BN	-9.2204	-3.4225	-5.0957
4	B	-7.8559	-1.7584	-6.6555
5	N	-8.3780	-0.8765	-6.0617
6	B	-6.3422	-7.9994	-6.8210
7	N	-6.4661	-7.3019	-4.9707
8	B	-7.8777	-1.9343	-6.5855
9	N	-7.6320	-1.0631	-6.1173

See Figures 1 and 2 for the rings and structures. BN: The perturbations occur at the fusion points of rings B and C. *: Failure occurred in the calculation.

4. Conclusion

In the present computational study, isomers of simultaneously boron and nitrogen-doped in adjacent positions of phenanthrene are considered within the restrictions of density functional theory and the applied basis set. In the vacuum conditions, all of them are characterized with exothermic heat of formations and

favorable Gibbs free energy of formation values and they are all electronically stable. All the HOMO and LUMO orbitals of the isomers possess π-symmetry and mostly localized on two adjacent atoms only. The perturbations in general raise up the HOMO but lower the LUMO energies as compared to the respective values of the parent phenanthrene system, depending on the localization of the perturbations. Thus the interfrontier molecular orbital gaps exhibit structural variations irregularly. Consequently, the UV-VIS spectra show bathochromic and hypsochromic shifts relatively among the isomers considered. The NICS values of the rings follow the algebraic order of A<C<B among the isomers. All the information presented here are ready for tailoring of scientists and engineers for special purposes of technological demands.

References

[1] Clar, E. (1972). *The aromatic sextet*. London: Wiley.

[2] Clar, E. (1964). *Polycyclic hydrocarbons*.1. London: Academic Press.

[3] Dewar, J.M.S. (1969). *The molecular orbital theory of organic chemistry*. New York: McGraw-Hill.

[4] Dewar, M.J.S., & Dougherty, R.C. (1975). *The PMO theory of organic chemistry*. New York: Plenum/Rosseta.

[5] Anslyn, E.V., & Dougherty, D.A. (2006). *Modern physical organic chemistry*. Sausalito, California: University Science Books.

[6] Stark, J.G. (2004). *Chemistry data book*. London: Hodder.

[7] Huang, H., Liu, L., Wang, J., Zhou, Y., Hu, H., Ye, Liu, X.G., Xu, Z., Xu, H., Yang, W., Wang, Y., Peng, Y., Yang, P., Sun, J., Yan, P., Cao, X., & Tang, B.Z. (2022). Aggregation caused quenching to aggregation induced emission transformation: a precise tuning based on BN-doped polycyclic aromatic hydrocarbons toward subcellular organelle specific imaging. *Chem. Sci*., *13*(11), 3129-3139. https://doi.org/10.1039/d2sc00380e

[8] Marwitz, A.J.V., Matus, M.H., Zakharov, L.N., Dixon, D.A., & Liu S.-Y. (2009). A hybrid organic/inorganic benzene. *Angew. Chem. Int. Ed*., *48*(5), 973-977. doi:10.1002/anie.200805554. PMID 19105174

[9] Wang, J-Y., & Pei, J. (2016). BN-embedded aromatics for optoelectronic applications. *Chinese Chemical Letters*, *27*(8), 1139-1146. https://doi.org/10.1016/j.cclet.2016.06.014

[10] Phukan, A., Kalagi, R., Gadre, S., & Jemmis, E. (2004). Structure, reactivity and aromaticity of acenes and their BN analogues: A density functional and electrostatic investigation. *Inorg. Chem*., *43*(19), 5824-5832. https://doi.org/10.1021/ic049690o

[11] Ito, S., Murata, T., Hasegawa, M., Bito, Y., Toyoguchi, Y. (1997). Study on C*x*N and C*x*S with disordered carbon structure as the anode materials for secondary lithium batteries. *J. Power Sources*, *68*(2), 245-248. https://doi.org/10.1016/S0378-7753(96)02588-8

[12] Endo, M., Kim, C., Karaki, T., Nishimura, Y., Matthews, M.J., & Brown, S.D.M. (1999). Anode performance of a Li ion battery based on graphitized and B-doped milled mesophase pitch-based carbon fibers. *Carbon*, *37*(4), 561-568. https://doi.org/10.1016/S0008-6223(98)00222-X

[13] Kurita, N., & Endo, M. (2002). Molecular orbital calculations on electronic and Li-adsorption properties of sulfur-, phosphorus- and silicon-substituted disordered carbons. *Carbon, 40*, 253-260. https://doi.org/10.1016/S0008-6223(01)00089-6

[14] Hasegawa, T., Suzuki, T., Mukai, R., & Tamon, H. (2004). Semi-empirical molecular orbital calculations on the Li ion storage states in heteroatom-substituted carbon materials. *Carbon, 42*(11), 2195-2200. https://doi.org/10.1016/j.carbon.2004.04.045

[15] Velinova, M., Georgiev, V., Todorova, T., Madjarova, G., Ivanova, A., & Tadjer, A. (2010). Boron-nitrogen- and boron-substituted anthracenes and phenanthrenes as models for doped carbon-based materials. *Journal of Molecular Structure: THEOCHEM*, *955* (1-3), 97-108. https://doi.org/10.1016/j.theochem.2010.06.003

[16] Sergeeva, A.P., Piazza, Z.A., Romanescu, C., Li, W-L., Boldyrev, A.I., & Wang, L-S. (2012). $B22^-$ and $B23^-$: All-boron analogues of anthracene and phenanthrene. *Journal of the American Chemical Society*, *134* (43), 18065-18073. https://doi.org/10.1021/ja307605t

[17] Greig, L.M., Kariuki, B.M., Habershon, S., Spencer, N., Johnston, R.L., Harris, K.D.M., & Philp, D. (2002). Solid-state and solution phase reactivity of 10-hydroxy-10,9-boroxophenanthrene: a model building block for self-assembly processes. *New J. Chem., 26*, 701-710. https://doi.org/10.1039/B110285K

[18] Pinheiro, M. Jr., Ferrão, L.F.A., Bettanin, F.A.J., Aquino, A., Machado, F.B.C., & Lischka, H. (2017). How to efficiently tune the biradicaloid nature of acenes by chemical doping with boron and nitrogen. *Phys. Chem. Chem. Phys*., *19*, 19225

[19] Yongkang, G., Chen, C., & Wang, X-Y. (2023). Recent advances in boron‐containing acenes: synthesis, properties, and optoelectronic applications. *Chinese Journal of Chemistry*, *41*(11), 1355-1373. https://doi.org/10.1002/cjoc.202200700

[20] Geffroy, B., le Roy, P., & Prat, C. (2006). Organic light-emitting diode (OLED) technology: materials, devices and display technologies. *Polym. Int*., *55*(6), 572-582. https://doi.org/10.1002/pi.1974

[21] Chen, H.-W., Lee, J.-H., Lin, B.-Y., Chen S., & Wu, S.-T. (2018). Liquid crystal, display and organic light-emitting diode display: present status and future perspectives. *Light Sci. Appl.*, *7*, 17168. https://doi.org/10.1038/lsa.2017.168

[22] Beaujuge, P.M., & Fréchet, J.M.J. (2011). Molecular design and ordering effects in π-functional materials for transistor and solar cell applications. *J. Am. Chem. Soc*., *133*(50), 20009-20029. https://doi.org/10.1021/ja2073643

[23] Cheng, P., Li, G., Zhan, X., & Yang, Y. (2018). Next-generation organic photovoltaics based on non-fullerene acceptors. *Nat. Photon*., *12*, 131-142 . https://doi.org/10.1038/s41566-018-0104-9

[24] Wu, W., Liu, Y., & Zhu, D. (2010). π-Conjugated molecules with fused rings for organic field-effect transistors: design, synthesis and applications. *Chem. Soc. Rev*., *39*, 1489-1502. https://doi.org/10.1039/B813123F

[25] Wang, C., Dong, H., Hu, W., Liu, Y., & Zhu, D. (2012). Semi conducting π-conjugated systems in field-effect transistors: A material odyssey of organic electronics. *Chemical Reviews, 112*(4), 2208-2267. https://doi.org/10.1021/cr100380z

[26] Sirringhaus, H. (2014). 25th Anniversary article: organic field-effect transistors: the path beyond amorphous silicon. *Adv. Mater*., *26* (9), 1319-1335. https://doi.org/10.1002/adma.201304346

[27] Chen, X., Tan, D., & Yang, D-T. (2022). Multiple-boron-nitrogen (multi-BN) doped π-conjugated systems for optoelectronic. *J. Mater. Chem. C*, *10*, 13499-13532. https://doi.org/10.1039/D2TC01106A

[28] Stewart, J.J.P. (1989). Optimization of parameters for semi-empirical methods I. *J. Comput. Chem.*, *10*, 209-220. https://doi.org/10.1002/jcc.540100208

[29] Stewart, J.J.P. (1989). Optimization of parameters for semi-empirical methods II. *J. Comput. Chem., 10*, 221-264. https://doi.org/10.1002/jcc.540100209

[30] Leach, A.R. (1997). *Molecular modeling*. Essex: Longman.

[31] Kohn, W., & Sham, L.J. (1965). Self-consistent equations including exchange and correlation effects. *Phys. Rev.*, *140*, 1133-1138. https://doi.org/10.1103/PhysRev.140.A1133

[32] Parr, R.G., & Yang, W. (1989). *Density functional theory of atoms and molecules*. London: Oxford University Press.

[33] Becke, A.D. (1988). Density-functional exchange-energy approximation with correct asymptotic behavior. *Phys. Rev. A*, *38*, 3098-3100. https://doi.org/10.1103/PhysRevA.38.3098

[34] Vosko, S.H., Wilk, L., & Nusair, M. (1980). Accurate spin-dependent electron liquid correlation energies for local spin density calculations: a critical analysis. *Can. J. Phys*., *58*, 1200-1211. https://doi.org/10.1139/p80-159

[35] Lee, C., Yang, W., & Parr, R.G. (1988). Development of the Colle-Salvetti correlation energy formula into a functional of the electron density. *Phys. Rev. B*, *37*, 785-789. https://doi.org/10.1103/PhysRevB.37.785

[36] SPARTAN 06 (2006). Wavefunction Inc. Irvine CA, USA.

[37] Gaussian 03, Frisch, M.J., Trucks, G.W., Schlegel, H.B., Scuseria, G.E., Robb, M.A., Cheeseman, J.R., Montgomery, Jr., J.A., Vreven, T., Kudin, K.N., Burant, J.C., Millam, J.M., Iyengar, S.S., Tomasi, J., Barone, V., Mennucci, B., Cossi, M., Scalmani, G., Rega, N., Petersson, G.A., Nakatsuji, H., Hada, M., Ehara, M., Toyota, K., Fukuda, R., Hasegawa, J., Ishida, M., Nakajima, T., Honda, Y., Kitao, O., Nakai, H., Klene, M., Li, X., Knox, J.E., Hratchian, H.P., Cross, J.B., Bakken, V., Adamo, C., Jaramillo, J., Gomperts, R., Stratmann, R.E., Yazyev, O., Austin, A.J., Cammi, R., Pomelli, C., Ochterski, J.W., Ayala, P.Y., Morokuma, K., Voth, G.A., Salvador, P., Dannenberg, J.J., Zakrzewski, V.G., Dapprich, S., Daniels, A.D., Strain, M.C., Farkas, O., Malick, D.K., Rabuck, A.D., Raghavachari, K., Foresman, J.B., Ortiz, J.V., Cui, Q., Baboul, A.G., Clifford, S., Cioslowski, J., Stefanov, B.B., Liu, G., Liashenko, A., Piskorz, P., Komaromi, I., Martin, R.L., Fox, D.J., Keith, T., Al-Laham, M.A., Peng, C.Y., Nanayakkara, A., Challacombe, M., Gill, P.M.W., Johnson, B., Chen, W., Wong, M.W., Gonzalez, C., & Pople, J.A., Gaussian, Inc., Wallingford CT, 2004.

[38] Fleming, I. (1976). *Frontier orbitals and organic reactions*. London: Wiley.

[39] Ferguson, L.N. (1969). *The modern structural theory of organic chemistry*. New Delhi: Prentice-Hall of India.

[40] Minkin, V.I., Glukhovtsev, M.N., & Simkin, B.Y. (1994). *Aromaticity and antiaromaticity: Electronic and structural aspects*. New York: Wiley.

[41] Schleyer, P.R., & Jiao, H. (1996). What is aromaticity?. *Pure Appl. Chem*., *68*, 209-218. https://doi.org/10.1351/pac199668020209

[42] Schleyer, P.R. (2001). Introduction: aromaticity. *Chem. Rev*., *101*, 1115-1118. https://doi.org/10.1021/cr0103221

[43] Cyranski, M.K., Krygowski, T.M., Katritzky, A.R., & Schleyer, P.R. (2002). To what extent can aromaticity be defined uniquely?. *J. Org. Chem*., *67*, 1333-1338. https://doi.org/10.1021/jo016255s

[44] Chen, Z., Wannere, C.S., Corminboeuf, C., Puchta, R., & Schleyer, P. von R. (2005). Nucleus independent chemical shifts (NICS) as an aromaticity criterion. *Chem. Rev.*, *105*(10), 3842-3888. https://doi.org/10.1021/cr030088

[45] Gershoni-Poranne, R., & Stanger, A. (2015). Magnetic criteria of aromaticity. *Chem., Soc. Rev*., *44*(18), 6597-6615. https://doi.org/10.1039/C5CS00114E

[46] Dickens, T.K., & Mallion, R.B. (2016). Topological ring-currents in conjugated systems. *MATCH Commun. Math. Comput. Chem*., *76*, 297-356.

[47] Stanger, A. (2010). Obtaining relative induced ring currents quantitatively from NICS. *J. Org. Chem*., *75*(7), 2281-2288. https://doi.org/10.1021/jo1000753

[48] Monajjemi, M., & Mohammadian, N.T. (2015). S-NICS: An aromaticity criterion for nano molecules. *J. Comput. Theor. Nanosci*., *12*(11), 4895-4914. https://doi.org/10.1166/jctn.2015.4458

[49] Schleyer, P.R., Maerker, C., Dransfeld, A., Jiao, H., & Hommes, N.J.R.E. (1996). Nucleus independent chemical shifts: a simple and efficient aromaticity probe. *J. Am. Chem. Soc*., *118*, 6317-6318. https://doi.org/10.1021/ja960582d

[50] Corminboeuf, C., Heine, T., & Weber, J. (2003). Evaluation of aromaticity: A new dissected NICS model based on canonical orbitals. *Phys. Chem. Chem. Phys.*, *5*, 246-251. https://doi.org/10.1039/B209674A

[51] Stanger, A. **(**2006). Nucleus-independent chemical shifts (NICS): Distance dependence and revised criteria for aromaticity and antiaromaticity. *The Journal of Organic Chemistry*, *71*(3), 883-893. https://doi.org/10.1021/jo051746o

[52] Chen, Z., Wannere, C.S., Corminboeuf, C., Puchta, R., & Schleyer, P.R. (2005). Nucleus-independent chemical shifts (NICS) as an aromaticity criterion. *Chemical Reviews*, *105*(10), 3842-3888. https://doi.org/10.1021/cr030088+